J. Fluid Mech. (1970), vol. 43, part 1, pp. 97–120
Printed in Great Britain

Internal waves in a wedge-shaped region

By D. G. HURLEY
Department of Mathematics, University of Western Australia

(Received 29 July 1969 and in revised form 31 March 1970)

The Green's functions are found for a line source of internal waves in a wedge of stratified fluid of constant Brunt–Väisälä frequency, and are used to discuss the diffraction of internal waves by a wedge in all cases when the vertex angle of the wedge of fluid exceeds the acute angle between a characteristic and the horizontal. Robinson's (1970) results are confirmed and extended.

It is found that the diffracted waves are as important as the incident and reflected ones at all points that lie within a quarter-wavelength or so of either characteristic that passes through the apex. Also, in cases when all the reflected waves are inclined forwards, the diffracted waves lead to a positive backscatter of energy. When the vertex angle of the fluid wedge is less than the characteristic angle, the diffraction problem appears to be ill-posed, and, instead, the motion due to a vibrating body in the wedge of fluid is considered.

A general conclusion is that the so-called ray theory for internal waves, in which the incident and reflected waves alone are considered, has similar limitations to the geometrical theory of optics. Both theories involve the assumption that the typical dimensions in the problem are large compared to the wavelength.

1. Introduction

Many of the properties of internal waves are quite different from those of the more well-known waves, such as light waves and sound waves. For example, according to the Boussinesq approximation, the phase and group velocities of internal waves are mutually perpendicular. To understand the behaviour of internal waves, it is highly desirable that there should be available an appreciable number of exact solutions that display their properties. The number of such solutions appears to be exceedingly small, even when the assumption of constant Brunt–Väisälä frequency is made. Robinson (1969) and Larson (1969) have solved the problem of an internal wave incident on a vertical barrier, and Wunsch (1968, 1969) has described certain special solutions involving internal waves in a wedge-shaped region.

Robinson (1970) gave the solution to the problem of an internal wave incident on a wedge for restricted values of the wedge angle. On being shown this solution, it was not at all apparent to the present author how it could be generalized to deal with more general wedge angles. This prompted the present investigation in which a somewhat different approach is taken.

In § 2 the Green's function is found for a source of waves in a wedge of arbitrary angle, and in subsequent sections it is used to discuss the diffraction of internal waves by wedges and a certain related problem for wedges of arbitrary angle.

The problem considered is also of some interest in oceanography in its own right, since, to a first approximation, the region near the foot of a suboceanic mountain range is an obtuse-angled wedge and the region above the continental shelf an acute-angled one.

2. Basic analysis

Suppose that stably stratified fluid, whose Brunt–Väisälä frequency,

$$N = \left(-\frac{1}{\rho_0}\frac{d\rho_0}{dy}\right)^{\frac{1}{2}}, \tag{2.1}$$

is constant, occupies the sector between two plane rigid walls OA and OB, OA being horizontal† and OB being inclined at an angle θ_B to it. Here ρ_0 is the undisturbed density, Oxy is a set of rectangular axes with Oy vertically upwards and θ_B may have any value in the range $(O, 2\pi)$.

Suppose, further, that motions are being produced in the fluid by oscillatory body forces whose components are $X \exp(-i\omega t)$ and $Y \exp(-i\omega t)$, where t is the time. Then Euler's equations of motion are

$$\frac{\partial u}{\partial t}+u\frac{\partial u}{\partial x}+v\frac{\partial u}{\partial y} = -\frac{1}{\rho}\frac{\partial p}{\partial x}+X\exp(-i\omega t), \tag{2.2}$$

$$\frac{\partial v}{\partial t}+u\frac{\partial v}{\partial x}+v\frac{\partial v}{\partial y} = -\frac{1}{\rho}\frac{\partial p}{\partial y}-g+Y\exp(-i\omega t)-\epsilon v, \tag{2.3}$$

the equation of continuity is

$$\frac{\partial \rho}{\partial t}+\frac{\partial}{\partial x}(\rho u)+\frac{\partial}{\partial y}(\rho v) = 0, \tag{2.4}$$

and the condition that the density of a fluid particle should remain constant gives

$$\frac{\partial \rho}{\partial t}+u\frac{\partial \rho}{\partial x}+v\frac{\partial \rho}{\partial y} = 0. \tag{2.5}$$

The term $-\epsilon v$ in (2.3) represents a small fictitious damping force proportional to the vertical velocity component, and is introduced for mathematical convenience. The solution of a particular physical problem is then the limit as ϵ tends to zero of the appropriate solution of (2.2) to (2.5). (See Lamb 1932, § 248.)

It may readily be shown that, if the motions are small and the Boussinesq approximation is made, the linear approximations to (2.2) to (2.5) imply that there exists a stream function $\psi \exp(-i\omega t)$, such that

$$u = -\frac{\partial \psi}{\partial y}\exp(-i\omega t), \quad v = \frac{\partial \psi}{\partial x}\exp(-i\omega t), \tag{2.6}$$

† This restriction is not essential. It is a trivial matter to generalize the analysis that follows to deal with cases when neither wall is horizontal.

and
$$\frac{\partial^2\psi}{\partial y^2}-\eta^2\frac{\partial^2\psi}{\partial x^2}=\frac{i}{\omega}\left(\frac{\partial Y}{\partial x}-\frac{\partial X}{\partial y}\right)=f(x,y),\quad \text{say,} \tag{2.7}$$

where
$$\eta^2=\frac{N^2}{\omega^2}-1-\frac{i\epsilon}{\omega}. \tag{2.8}$$

ψ must also satisfy the boundary conditions,

$$\psi=0 \quad \text{on} \quad \theta=0,\theta_B, \qquad 0<r<\infty, \tag{2.9}$$

where r, θ are polar co-ordinates.

We note that the homogeneous form of (2.7) implies that both the real and imaginary parts of ψ satisfy

$$\left\{\left(\frac{N^2}{\omega^2}-1\right)^2+\frac{\epsilon^2}{\omega^2}\right\}\frac{\partial^4 h}{\partial x^4}-2\left(\frac{N^2}{\omega^2}-1\right)\frac{\partial^4 h}{\partial x^2\,\partial y^2}+\frac{\partial^4 h}{\partial y^4}=0. \tag{2.10}$$

This equation is elliptic if $\epsilon \neq 0$, so that then ψ will be regular in both x and y (see, for example, Bers *et al.* 1964, p. 136), and analytic continuation may be used to extend its range of definition, a procedure we will employ frequently in what follows.

Under the transformation

$$\left.\begin{aligned} x &= e^\rho\cos\phi, & \eta y &= e^\rho\sin\phi,\\ \tan\phi &= \eta\tan\theta, & \rho &= \tfrac{1}{2}\log(x^2+\eta^2y^2),\end{aligned}\right\} \tag{2.11}$$

(2.7) becomes

$$-\frac{\partial^2\psi}{\partial\rho^2}+2\tan 2\phi\frac{\partial^2\psi}{\partial\rho\,\partial\phi}+\frac{\partial^2\psi}{\partial\phi^2}+2\frac{\partial\psi}{\partial\rho}-2\tan 2\phi\frac{\partial\psi}{\partial\phi}=\frac{f(\rho,\phi)\exp 2\rho}{\eta^2\cos 2\phi}. \tag{2.12}$$

Let
$$\overline{\psi}=\frac{1}{\sqrt{(2\pi)}}\int_{-\infty}^{\infty}\psi\exp(iw\rho)\,d\rho \tag{2.13}$$

be the Fourier transform of ψ with respect to ρ. Then (2.12) implies

$$\frac{d}{d\phi}\left\{(\cos 2\phi)^{1+iw}\frac{\partial\overline{\psi}}{d\phi}\right\}+w(w-2i)(\cos 2\phi)^{1+iw}\overline{\psi}=-F(w), \tag{2.14}$$

where
$$F(w)=-\frac{(\cos 2\phi)^{iw}}{\sqrt{(2\pi)}\,\eta^2}\int_{-\infty}^{\infty}f(\rho,\phi)\exp[\rho(2+iw)]\,d\rho. \tag{2.15}$$

Also, the boundary conditions (2.9) become

$$\overline{\psi}=0 \quad \text{on} \quad \phi=0 \quad \text{and on} \quad \phi=\phi_B=\operatorname{artan}(\eta\tan\theta_B). \tag{2.16}$$

The general solution of the homogeneous form of (2.14) is

$$\begin{aligned}\overline{\psi}&=c_1(1+\sin 2\phi)^{-\frac{1}{2}(iw)}+c_2(1-\sin 2\phi)^{-\frac{1}{2}(iw)}\\ &=c_1\exp\{iw\rho-iw\log(x+\eta y)\}+c_2\exp\{iw\rho-iw\log(x-\eta y)\},\end{aligned} \tag{2.17}$$

using (2.11). Here, $\log(x+\eta y)$ and $\log(x-\eta y)$ have branch points for $x+\eta y=0$ and $x-\eta y=0$. Each is taken to have its principal value on the positive Ox axis and analytic continuation, as described above, may be employed to determine the values throughout the Oxy plane. Thus,

$$\log(x+\eta y)=\log|x+\eta y|-im\pi,$$

and
$$\log(x-\eta y)=\log|x-\eta y|+in\pi,$$

where

$$\begin{aligned} m &= 0, & 0 &< \theta < \pi-\mu, \\ &= 1, & \pi-\mu &< \theta < 2\pi-\mu, \\ &= 2, & 2\pi-\mu &< \theta < 2\pi, \\ n &= 0, & 0 &< \theta < \mu, \\ &= 1, & \mu &< \theta < \pi+\mu, \\ &= 2, & \pi+\mu &< \theta < 2\pi, \end{aligned} \tag{2.18}$$

and

$$\mu = \operatorname{arccot} \eta. \tag{2.19}$$

By using conventional methods (see, for example, Sagan 1961, ch. IX), it can be shown that the Green's function $\bar{G}(\phi, \phi_S; w)$ for (2.14), subject to (2.16), is given by

$$\bar{G}(\phi, \phi_S; w)(\cos 2\phi_S)^{iw} \exp[-iw(\rho-\rho_S)]$$

$$= \frac{i[(x+\eta y)^{-iw}-(x-\eta y)^{-iw}]\left[(x_S-\eta y_S)^{iw}-\left\{\dfrac{(x_S+\eta y_S)(x_B-\eta y_B)}{x_B+\eta y_B}\right\}^{iw}\right]}{2w\left[1-\left\{\dfrac{x_B-\eta y_B}{x_B+\eta y_B}\right\}^{iw}\right]}, \quad \phi < \phi_S,$$

$$= \frac{i\left[(x+\eta y)^{-iw}-\left\{\dfrac{(x-\eta y)(x_B+\eta y_B)}{x_B-\eta y_B}\right\}^{-iw}\right][(x_S-\eta y_S)^{iw}-(x_S+\eta y_S)^{iw}]}{2w\left[1-\left\{\dfrac{x_B-\eta y_B}{x_B+\eta y_B}\right\}^{iw}\right]}, \quad \phi > \phi_S, \tag{2.20}$$

where subscript B denotes values at any point on OB and subscript S values at a 'source' point.

It follows, from (2.7), (2.11) and the inversion formula for Fourier integrals, that ψ is given in terms of $\bar{G}$ by

$$\psi = \int\int_R \left(\frac{\partial Y}{\partial x_S} - \frac{\partial X}{\partial y_S}\right) \psi_V(x, y; x_S, y_S)\, dx_S\, dy_S, \tag{2.21}$$

where

$$\psi_V(x, y; x_S, y_S) = \frac{-i}{2\pi\omega\eta}\int_{-\infty}^{\infty} \bar{G}(\phi, \phi_S; w)(\cos 2\phi_S)^{iw} \exp[-iw(\rho-\rho_S)]\, dw. \tag{2.22}$$

For all values of ϕ, the expression (2.20) has simple poles at

$$w_n = 2n\pi/C \quad (n = \pm 1, \pm 2, \ldots), \tag{2.23}$$

where

$$C = \log\left(\frac{x_B+\eta y_B}{x_B-\eta y_B}\right) = \log|K| - i(m_B+n_B)\pi, \tag{2.24}$$

and

$$K = \frac{\sin(\theta_B+\mu)}{\sin(\theta_B-\mu)}, \tag{2.25}$$

with residues

$$R_n = \frac{-i}{8\pi^2\omega\eta n}\{(x+\eta y)^{-iw_n}-(x-\eta y)^{-iw_n}\}\{(x_S-\eta y_S)^{iw_n}-(x_S+\eta y_S)^{iw_n}\}. \tag{2.26}$$

To evaluate (2.22) consider the case† $0 < \theta_B < \mu$. Then, with η given by (2.8) the poles (2.23) lie close to the real axis in the first and third quadrants. When $\rho < \rho_S$, the contribution to the integral from a large semicircle in the upper half plane is small, so that, by Cauchy's theorem,

$$\psi_V = 2\pi i \sum_{n=1}^{\infty} R_n \tag{2.27}$$

$$= \frac{1}{4\pi\omega\eta} \log \frac{(1-\exp(-i\alpha_1))(1-\exp(-i\alpha_2))}{(1-\exp(-i\alpha_3))(1-\exp(-i\alpha_4))}, \tag{2.28}$$

where

$$\left.\begin{aligned} \alpha_1 &= \frac{2\pi}{C}\log\left(\frac{x+\eta y}{x_S+\eta y_S}\right), \quad \alpha_2 = \frac{2\pi}{C}\log\left(\frac{x-\eta y}{x_S-\eta y_S}\right), \\ \alpha_3 &= \frac{2\pi}{C}\log\left(\frac{x+\eta y}{x_S-\eta y_S}\right), \quad \alpha_4 = \frac{2\pi}{C}\log\left(\frac{x-\eta y}{x_S+\eta y_S}\right), \end{aligned}\right\} \tag{2.29}$$

and use has been made of the result

$$\sum_{n=1}^{\infty} \frac{\exp(in\theta)}{n} = -\log(1-\exp(i\theta)). \tag{2.30}$$

If $\rho > \rho_S$,

$$\psi_V = -2\pi i \sum_{n=-1}^{-\infty} R_n, \tag{2.31}$$

and the use of (2.30) again leads to (2.28). The identity of the two results is expected, since ψ_V satisfies the elliptic equation (2.10), and is thus regular in x and y.

To demonstrate that the expression (2.28) for ψ_V is unique, we must show that the homogeneous form of (2.12) has no non-trivial acceptable solutions. Now (2.17) satisfies (2.16), only if

$$w = w_n, \quad n = \pm 1, \pm 2, \ldots, \tag{2.32}$$

where w_n is given by (2.23). These values of w give rise to the eigensolutions R_n given by (2.26), so that the most general solution of the homogeneous form of (2.12) that satisfies (2.9) is

$$\psi_H = \sum_{n=-\infty}^{\infty}{}' a_n R_n. \tag{2.33}$$

Now, if $\theta_B > \mu$, $-2\pi i/C$ has positive real part (except if θ_B equals $\pi \pm \mu$ or $2\pi - \mu$, in which case the real part is zero), and, referring to (2.26), we see that R_n tends to infinity as $x \pm \eta y$ tends to infinity, if $n \geqslant 1$, and tends to infinity as $x \pm \eta y$ tends to zero, if $n \leqslant -1$. Since ψ must be bounded in each of these limits, all the a_n in (2.33) must vanish. Hence, (2.28) gives the unique solution.

If $0 < \theta_B < \mu$, $-2\pi i/C$ is pure imaginary if the damping coefficient ϵ in (2.8) is zero. However, if $\epsilon > 0$, $-2\pi i/C$ has a positive real part, and similar arguments to those used above again give $\psi_H \equiv 0$.

Equations (2.21) and (2.28) give the desired solution for an arbitrary distribution of body forces.

† It may easily be verified that the resulting expression for ψ_V, given by (2.28), satisfies all the required conditions and thus constitutes the solution to the problem for all values of θ_B.

3. Diffraction of internal waves by a wedge

Suppose now that at large distances from the apex of the wedge of stratified fluid there exists an incident wave

$$\psi_i = U \exp[ik(x \sin\theta + y\cos\theta)]/k, \tag{3.1}$$

where k is positive. Since time variations are given by the factor $\exp(-i\omega t)$, the phase velocity of the wave $\tilde{C}_{P_i}$ has magnitude ω/k, and is in the direction of the wave-number vector,

$$(k_1, k_2) = (k\sin\theta, k\cos\theta). \tag{3.2}$$

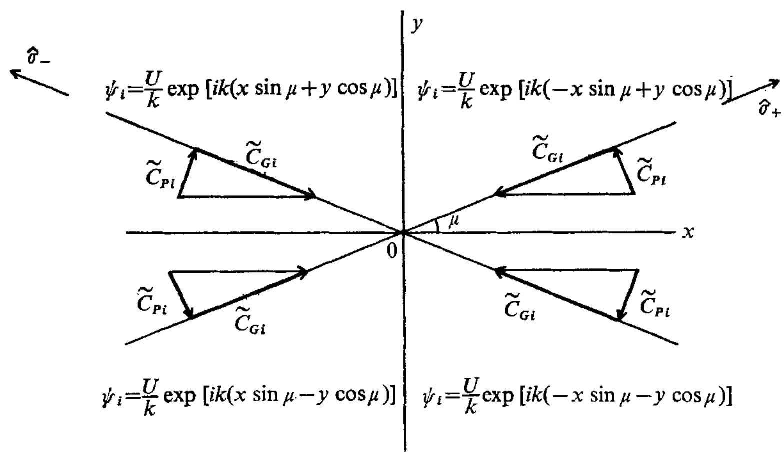

FIGURE 1. The phase and group velocities of the four possible incident waves

$$\psi_i = U \exp[ik(\pm x \sin\mu \pm y\cos\mu)]/k,$$

and definition of the unit vectors $\hat{\sigma}_+$ and $\hat{\sigma}_-$.

The condition that (3.1) should satisfy the homogeneous form of (2.7), and thus represent a possible wave, is

$$\cot^2\theta = \cot^2\mu, \tag{3.3}$$

where μ is the acute angle defined by (2.19) and (2.8) with $\epsilon = 0$. Equation (3.3) will be satisfied provided

$$\cos\theta = \pm\cos\mu \quad \text{and} \quad \sin\theta = \pm\sin\mu. \tag{3.4}$$

Thus, for given μ, there are four possible incident waves that are represented by

$$\psi_i = U\exp[ik(\pm x\sin\mu \pm y\cos\mu)]/k. \tag{3.5}$$

The group velocity $\tilde{C}_{G_i}$ of each of the waves (3.5) has magnitude $N\cos\mu/k$, and is perpendicular to $\tilde{C}_{P_i}$ in the sense such that the horizontal components of $\tilde{C}_{P_i}$ and $\tilde{C}_{G_i}$ have the same sign. (See Phillips 1966, p. 175.) Figure 1 shows the phase and group velocities of each of the four waves given by (3.5). We shall describe the analysis for the case

$$\psi_i = U\exp[-ik(x\sin\mu - y\cos\mu)]/k, \tag{3.6}$$

but only minor changes would be needed to deal with the other cases.

The problem of the diffraction of an internal wave by a wedge has recently been treated by Robinson (1970) for the incident wave (3.6) and the case $\mu < \theta_B < \pi - \mu$. In §3 we shall use the results of §2 to derive his solution in a form that holds provided only that

$$\mu < \theta_B < 2\pi. \tag{3.7}$$

The case $0 < \theta_B < \mu$ will be considered in §5.

The fluid velocity corresponding to (3.6) is

$$-iU\hat{\sigma}_+ \exp\left[-ik(x\sin\mu - y\cos\mu)\right], \tag{3.8}$$

so that U is the amplitude of the velocity fluctuation in the incident wave and the unit vector $\hat{\sigma}_+$ is defined in figure 1.

The stream function for the total motion is written

$$\Psi = \psi_i + \psi, \tag{3.9}$$

where ψ must satisfy the homogeneous form of (2.7) and the boundary conditions

$$\psi = -U\exp(-ikr\sin\mu)/k \quad (\theta = 0, \quad 0 < r < \infty),$$

$$\text{and} \qquad \psi = -U\exp\left[-ikr\sin(\mu - \theta_B)\right]/k \quad (\theta = \theta_B, \quad 0 < r < \infty). \tag{3.10}$$

We now show that ψ can be expressed in terms of a distribution of sources on OA and OB.

If ψ_V as given by (2.28) is multiplied by $-i\omega\eta^2/2$, integrated with respect to y_S and differentiated with respect to x_S, the result is the stream function,

$$\psi_S = -\frac{i}{8\pi}\log\left[\frac{(1-\exp[-i\alpha_1])(1-\exp[-i\alpha_3])}{(1-\exp[-i\alpha_2])(1-\exp[-i\alpha_4])}\right]. \tag{3.11}$$

α_1, α_2, α_3 and α_4 are given by (2.29); and from this equation and (3.11) it follows that

$$\psi_S \doteqdot -\frac{i}{4\pi}\log\left(\frac{x+\eta y - x_S - \eta y_S}{x - \eta y - x_S + \eta y_S}\right), \tag{3.12}$$

provided the field point (x, y) is close to the point (x_S, y_S), at which the singularity is located. Equation (3.17) of Hurley (1969) shows that (3.12) gives the stream function for a source of strength $\cos\omega t$ at the point (x_S, y_S) in unbounded stratified fluid, so that (3.11) gives the flow due to the same source with the lines $\theta = 0$ and $\theta = \theta_B$ streamlines.

Taking $x_S = t_A$, $y_S = 0$ in (2.29) and (3.11) gives a unit source on OA:

$$\left.\begin{aligned} \psi_A &= \frac{i}{4\pi}\log\left(\frac{1-\exp(-i\alpha_+)}{1-\exp(-i\alpha_-)}\right), \\ \text{where} \quad \alpha_+ &= \frac{2\pi}{C}\log\left(\frac{x-\eta y}{t_A}\right), \quad \text{and} \quad \alpha_- = \frac{2\pi}{C}\log\left(\frac{x+\eta y}{t_A}\right). \end{aligned}\right\} \tag{3.13}$$

Taking $x_S = t_B\cos\theta_B$, $y_S = t_B\sin\theta_B$ gives a unit source on OB:

$$\left.\begin{aligned} \psi_B &= \frac{i}{4\pi}\log\left(\frac{1-\exp[-i\beta_+]}{1-\exp[-i\beta_-]}\right), \\ \text{where} \quad \beta_+ &= \frac{2\pi}{C}\log\left(\frac{x-\eta y}{t_B(1+v_B)\cos\theta_B}\right), \quad \beta_- = \frac{2\pi}{C}\log\left(\frac{x+\eta y}{t_B(1+v_B)\cos\theta_B}\right) \\ \text{and} \quad v_B &= \eta\tan\theta_B. \end{aligned}\right\} \tag{3.14}$$

Now ψ_A gives a normal velocity $\frac{1}{2}\delta(r-t_A)$ on $\theta = 0$ and ψ_B a normal velocity $\frac{1}{2}\delta(r-t_B)$ on $\theta = \theta_B$ (see Hurley 1969, §4) where δ denotes the Dirac delta function. Thus, by (3.10), (3.13) and (3.14),

$$\psi = \psi_1+\psi_2+\psi_3+\psi_4,$$

where

$$\left.\begin{aligned}
\psi_1 &= -\frac{U\sin\mu}{2\pi k}\int_0^\infty \exp[-i\tau_A\sin\mu]\log\left(1-\exp\left[-\frac{2\pi i}{C}\log\left(\frac{k(x-\eta y)}{\tau_A}\right)\right]\right)d\tau_A,\\
\psi_2 &= \frac{U\sin\mu}{2\pi k}\int_0^\infty \exp[-i\tau_A\sin\mu]\log\left(1-\exp\left[-\frac{2\pi i}{C}\log\left(\frac{k(x+\eta y)}{\tau_A}\right)\right]\right)d\tau_A,\\
\psi_3 &= -\frac{U\sin(\theta_B-\mu)}{2\pi k}\int_0^\infty \exp[i\tau_B\sin(\theta_B-\mu)]\\
&\qquad\times\log\left(1-\exp\left[-\frac{2\pi i}{C}\log\left(\frac{k(x-\eta y)}{\tau_B(1+v_B)\cos\theta_B}\right)\right]\right)d\tau_B,\\
\psi_4 &= \frac{U\sin(\theta_B-\mu)}{2\pi k}\int_0^\infty \exp[i\tau_B\sin(\theta_B-\mu)]\\
&\qquad\times\log\left(1-\exp\left[-\frac{2\pi i}{C}\log\left(\frac{k(x+\eta y)}{\tau_B(1+v_B)\cos\theta_B}\right)\right]\right)d\tau_B
\end{aligned}\right\}\quad(3.15)$$

and the changes of variables,

$$\tau_A = kt_A, \quad\text{and}\quad \tau_B = kt_B \qquad (3.16)$$

have been made.

Each of the above integrals is of the type

$$I = \int_0^\infty \exp(iRt)\log\left(1-\exp\left[-\frac{2\pi i}{C}\log\frac{q}{t}\right]\right)dt, \qquad (3.17)$$

where, in the case $\epsilon = 0$, R is real and

$$\log q = \log|q| + is\pi, \qquad (3.18)$$

where s is a positive or negative integer of zero.

The only singularities of the integrand in (3.17) are branch points which occur for

$$\log q/t = NC \quad (N = 0, \pm 1, \ldots),$$

or, by (2.24),

$$t = |q|\,|K|^{-N}, \qquad (3.19)$$

and

$$\operatorname{amp} t = \pi\{s+N(m_B+n_B)\}.$$

Since the above value for amp t is an integral multiple of π, all the branch points lie on the real axis.

In the case $\epsilon \neq 0$, η is given by (2.8) and then each q and the branch points given by (3.19) acquire imaginary parts. Let a_j $(j = 1, 2, \ldots, r)$ be the location of those that are displaced into the first quadrant and b_j $(j = 1, 2, \ldots, s)$ be the location of those that are displaced into the fourth quadrant. Then it follows from Jordan's lemma and Cauchy's theorem that

$$\left.\begin{aligned}
I &= \int_0^{0+i\infty} F(t)\,dt + \int_{\sum_{j=1}^{r} c_j} F(t)\,dt \quad (R>0),\\
&= \int_0^{0-i\infty} F(t)\,dt + \int_{\sum_{j=1}^{s} \Gamma_j} F(t)\,dt \quad (R<0),
\end{aligned}\right\}\quad(3.20)$$

where
$$F(t) = \exp(iRt)\log\left(1-\exp\left[-\frac{2\pi i}{C}\log\frac{q}{t}\right]\right), \tag{3.21}$$
and the contours C_j and Γ_j are depicted in figure 2.

The integrals along C_j and Γ_j can be resolved exactly. For on C_j,
$$\log\left(1-\exp\left[-\frac{2\pi i}{C}\log\frac{q}{t}\right]\right) = \log(t-a_j)+f(t), \tag{3.22}$$
where $f(t)$ is regular on C_j, and hence does not contribute to the integral. This result, and the corresponding one for Γ_j, give
$$\int_{C_j} F(t)\,dt = -\frac{2\pi}{R}\exp(iRa_j) \quad (R > 0), \tag{3.23}$$
and
$$\int_{\Gamma_j} F(t)\,dt = \frac{2\pi}{R}\exp(iRb_j) \quad (R < 0).$$

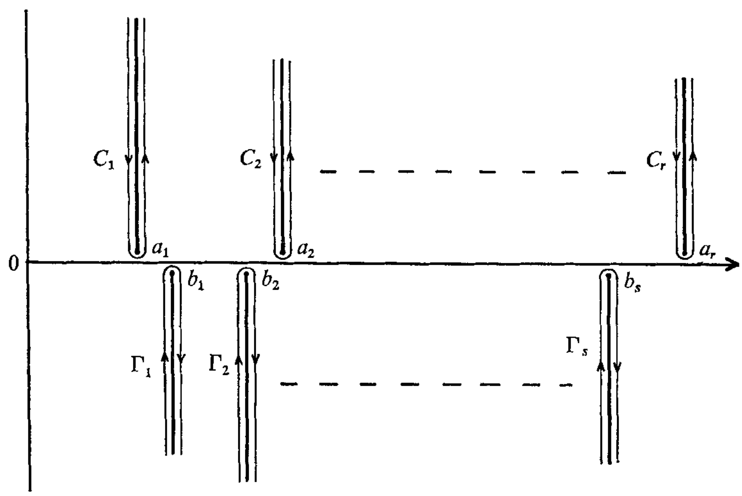

FIGURE 2. Definition of contours C_j and Γ_j.

3.1. *The reflected waves*

ψ, as given by (3.15), consists of a linear combination of four integrals of the type (3.17). We now calculate the contributions to these integrals from the contours C_j or Γ_j and find that these represent the reflected waves.

Let $\psi_{p\mathscr{R}}$, $p = 1, 2, 3, 4$, denote the contribution to ψ_p from the contour C_j or Γ_j, as the case may be. Consider $\psi_{1\mathscr{R}}$. Equations (3.17) and (3.18) show that for $\epsilon = 0$,
$$R = -\sin\mu, \quad q = k(x-\eta y), \quad \text{and} \quad s = n, \tag{3.24}$$
by (2.18). The conditions (3.19) for branch points are therefore
$$t = k|x-zy|\,|K|^{-N} \quad (N = 0, \pm 1, \ldots), \tag{3.25}$$
and
$$n = -N(m_B+n_B).$$
Since $n_B \geqslant 1$ and $n_B \geqslant n$, the only values of N for which the second of equations (3.25) may be satisfied are $N = 0$ and $N = -1$. If $N = 0$, then $n = 0$, so that $0 < \theta < \mu$, and the branch point is at
$$t = k(x-\eta y). \tag{3.26}$$

Term in equation (3.15)	Contribution(s)	Condition under which contribution occurs	Region in which contribution occurs	Physical interpretation of contribution
ψ_1	$U \exp [ikK(x \sin \mu - y \cos \mu)]/k$	$\mu < \theta_B < \pi - \mu$	$\mu < \theta < \theta_B$	$\psi_{\mathscr{R}AB}$
ψ_2	$-U \exp [-ik(x \sin \mu + y \cos \mu)]/k$	Occurs under all conditions	$0 < \theta <$ smaller of θ_B and $\pi - \mu$	$\psi_{\mathscr{R}A}$
ψ_3	$U \exp \left[\frac{ik}{K}(x \sin \mu - y \cos \mu)\right] \Big/ k$	$\mu < \theta_B < \pi - \mu$	$0 < \theta < \mu$	$\psi_{\mathscr{R}BA}$
	$-U \exp [-ik(x \sin \mu - y \cos \mu)]/k$	$\theta_B > \pi + \mu$	$\pi + \mu < \theta < \theta_B$	$-\psi_i$
ψ_4	$-U \exp \left[\frac{ik}{K}(x \sin \mu + y \cos \mu)\right] \Big/ k$	$\theta_B < \pi + \mu$	$0 < \theta < \theta_B$ if $\theta_B < \pi - \mu$ $\pi - \mu < \theta < \theta_B$ if $\theta_B > \pi - \mu$	$\psi_{\mathscr{R}B}$

TABLE 1. The contributions of the various terms in equation (3.15) to the reflected waves for $\psi_i = U \exp [-ik(x \sin \mu - y \cos \mu)]/k$ and $\mu < \theta_B < 2\pi$.

If $N = -1$, then $n = m_B + n_B$ or $n = n_B = 1$, and $m_B = 0$. The conditions $m_B = 0$, $n_B = 1$ imply $\mu < \theta_B < \pi - \mu$, and the condition $n = 1$ implies $\mu < \theta < \theta_B$. The branch point is at

$$t = kK(\eta y - x). \tag{3.27}$$

Now for $\epsilon \neq 0$, η is given by (2.8), and then the branch point (3.26) acquires a positive imaginary part and branch point (3.27) a negative one. Since $R = -\sin\mu$ is negative, a contribution to $\psi_{1\mathscr{R}}$ is obtained from the branch point (3.27), but not from the branch point (3.26). Hence, if

$$\mu < \theta_B < \pi - \mu, \tag{3.28}$$

$$\begin{aligned} \psi_{1\mathscr{R}} &= (U/k)\exp[ikK(x\sin\mu - y\cos\mu)], \quad \text{in} \quad \mu < \theta < \theta_B, \\ &= 0 \quad \text{elsewhere.} \end{aligned} \tag{3.29}$$

If the inequality (3.28) is not satisfied, then $\psi_{1\mathscr{R}} \equiv 0$. The values of $\psi_{p\mathscr{R}}$, $p = 2, 3, 4$ may be obtained in a similar way, and are given in table 1.

The laws of reflexion for an internal wave by an *infinite* plane are given by Phillips (1966, p. 176), and, using these, it is a simple matter to establish the physical interpretation given in the last column of the table of the various terms. Here $\psi_{\mathscr{R}A}(\psi_{\mathscr{R}B})$ denotes the reflected wave, if the wave ψ_i is incident on the face $OA(OB)$. $\psi_{\mathscr{R}AB}$ denotes the reflected wave, if the wave $\psi_{\mathscr{R}A}$ is incident on the face OB, and $\psi_{\mathscr{R}BA}$ denotes the reflected wave, if the wave $\psi_{\mathscr{R}B}$ is incident on the face OA.

Figure 3 depicts the sum of the incident and reflected waves for various values of θ_B. The arrows in the figure are drawn in the directions of the group-velocities of the various waves and it is seen that in each case a particular wave is found in those regions that can be reached by rays whose direction at any point is that of the appropriate group velocity.

3.2. *The diffracted waves*

The stream function $\psi_{\mathscr{D}}$ for the diffracted waves consists of the contributions to the integrals in (3.15) from the paths along the positive or negative imaginary axes. Using the changes of variable,

$$\left.\begin{aligned} \tau_A &= -it_A, \\ \tau_B &= \pm it_B, \ \sin(\theta_B - \mu) \gtrless 0, \end{aligned}\right\} \tag{3.30}$$

it is found that

$$\left.\begin{aligned} \psi_{\mathscr{D}} = &-\frac{iU\sin\mu}{2\pi k}\int_0^\infty \exp[-t_A\sin\mu]\log\left\{\frac{1-\exp\left[-\dfrac{2\pi i}{C}\log\left(\dfrac{k(x+\eta y)}{-it_A}\right)\right]}{1-\exp\left[-\dfrac{2\pi i}{C}\log\left(\dfrac{k(x-\eta y)}{-it_A}\right)\right]}\right\}dt_A \\ &+\frac{iU|\sin(\theta_B-\mu)|}{2\pi k}\int_0^\infty \exp[-t_B|\sin(\theta_B-\mu)|] \\ &\times\log\left\{\frac{1-\exp\left[-\dfrac{2\pi i}{C}\log\left(\dfrac{k(x+\eta y)}{\pm it_B(1+v_B)\cos\theta_B}\right)\right]}{1-\exp\left[-\dfrac{2\pi i}{C}\log\left(\dfrac{k(x-\eta y)}{\pm it_B(1+v_B)\cos\theta_B}\right)\right]}\right\}dt_B, \ \sin(\theta_B-\mu)\gtrless 0. \end{aligned}\right\} \tag{3.31}$$

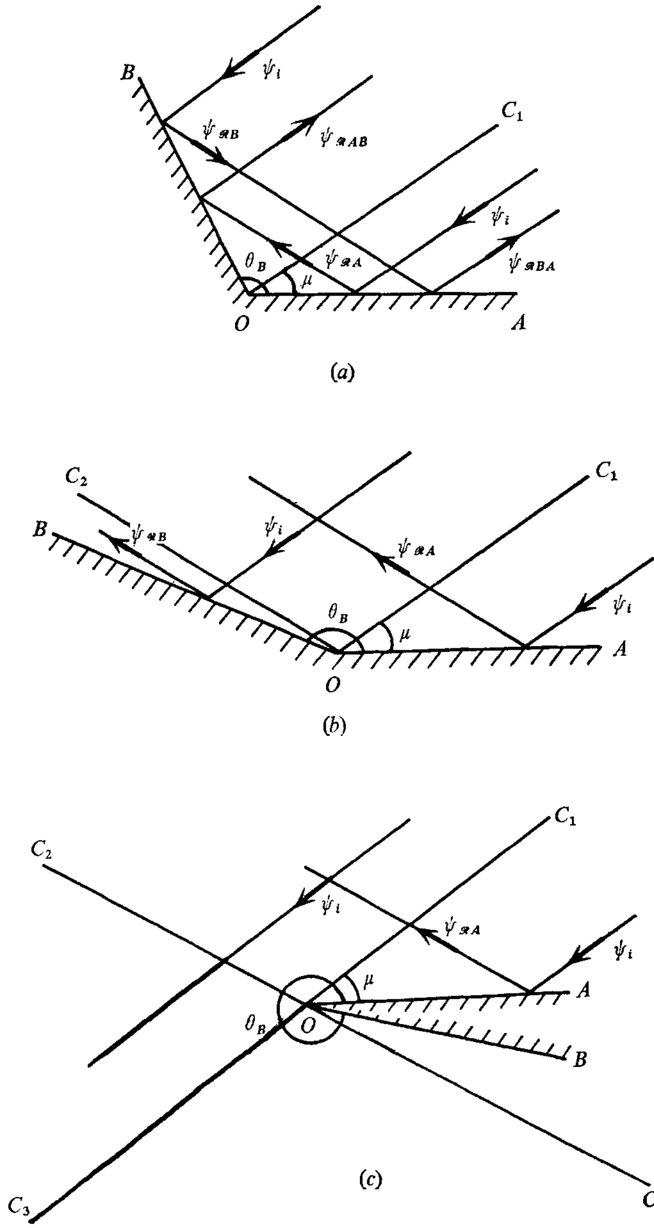

FIGURE 3. The incident and reflected waves for various values of θ_B. The arrows are drawn in the direction of the group velocity:

(*a*) $\mu < \theta_B < \pi-\mu$. The incident and reflected waves consist of: ψ_i, $0 < \theta < \theta_B$; $\psi_{\mathscr{R}A}$, $0 < \theta < \theta_B$; $\psi_{\mathscr{R}B}$, $0 < \theta < \theta_B$; $\psi_{\mathscr{R}AB}$, $\mu < \theta < \theta_B$ and $\psi_{\mathscr{R}BA}$, $0 < \theta < \mu$.

(*b*) $\pi-\mu < \theta_B < \pi+\mu$. The incident and reflected waves consist of: ψ_i, $0 < \theta < \theta_B$; $\psi_{\mathscr{R}A}$, $0 < \theta < \pi-\mu$ and $\psi_{\mathscr{R}B}$, $\pi-\mu < \theta < \theta_B$.

(*c*) $\pi+\mu < \theta_B < 2\pi$. The incident and reflected waves consist of: ψ_i, $0 < \theta < \pi+\mu$ and $\psi_{\mathscr{R}A}$, $0 < \theta < \pi-\mu$.

We express $\psi_{\mathscr{D}}$ in the form

$$\psi_{\mathscr{D}} = \psi_{\mathscr{D}+}(\sigma_+) + \psi_{\mathscr{D}-}(\sigma_-), \tag{3.32}$$

where

$$\left.\begin{aligned}\sigma_+ &= x\sin\mu - y\cos\mu,\\ \sigma_- &= x\sin\mu + y\cos\mu,\end{aligned}\right\} \tag{3.33}$$

so that the velocity in the diffracted wave is

$$\psi'_{\mathscr{D}+}\hat{\sigma}_+ + \psi'_{\mathscr{D}-}\hat{\sigma}_-, \tag{3.34}$$

where the unit vectors $\hat{\sigma}_+$ and $\hat{\sigma}_-$ are defined in figure 1.

Now (3.31) gives $\psi_{\mathscr{D}-}$ as the sum of two functions and, if the changes of variable,

$$\frac{t_A}{k|x+\eta y|} = t \quad\text{and}\quad \frac{t_B}{k}\left|\frac{(1-v_B)\cos\theta_B}{x+\eta y}\right| = t, \tag{3.35}$$

are made, it is found, after a little reduction, that

$$\psi'_{\mathscr{D}-} = \frac{U\operatorname{sgn}\sigma_-}{C}\sinh\left(\frac{\pi^2}{C}\left[n_B+\begin{matrix}1\\0\end{matrix}\right]\right)$$
$$\times\int_0^\infty \frac{\exp(-k|\sigma_-|t)\,dt}{\cos\left(\dfrac{\pi}{C}\left[2\log t + i\pi\left(2m+n_B-\begin{matrix}0\\1\end{matrix}\right)\right]\right)-\cosh\left(\dfrac{\pi^2}{C}\left[n_B+\begin{matrix}1\\0\end{matrix}\right]\right)},\ \sin(\theta_B-\mu)\gtrless 0. \tag{3.36}$$

Similarly,

$$\psi'_{\mathscr{D}+} = -\frac{U\operatorname{sgn}\sigma_+}{C}\sinh\left(\frac{\pi^2}{C}\left[n_B+\begin{matrix}1\\0\end{matrix}\right]\right)$$
$$\times\int_0^\infty \frac{\exp(-k|\sigma_+|t)\,dt}{\cos\left(\dfrac{\pi}{C}\left[2\log t + i\pi\left(-2n+n_B-\begin{matrix}0\\1\end{matrix}\right)\right]\right)-\cosh\left(\dfrac{\pi^2}{C}\left[n_B+\begin{matrix}1\\0\end{matrix}\right]\right)},\ \sin(\theta_B-\mu)\gtrless 0. \tag{3.37}$$

4. Numerical results and discussion for case $\theta_B > \mu$

Equations (3.36) and (3.37) give the velocities in the diffracted waves for all points in the wedge of fluid and for all values of $\theta_B > \mu$. m and n therein are given by (2.18), and in general these, and hence the fluid velocities, are discontinuous across the characteristics $x \pm \eta y = 0$ that pass through the apex of the wedge.

Dependence on θ_B occurs through

$$-2\pi i/C = \alpha = \alpha_1 + i\alpha_2, \quad\text{say,} \tag{4.1}$$

where C is given by (2.24). Values of α are given in figure 4, where without loss of generality, and to facilitate discussion, we have taken $\mu = \frac{1}{4}\pi$.

The figure shows that

$$\alpha_1 > 1, \tag{4.2}$$

if $0{\cdot}829 < \theta_B < 2{\cdot}313$ approximately, and, for these values of θ_B, the fluid velocities in the diffracted wave will be bounded on the line $x - \eta y = 0$ (Robinson 1970). For all other values of θ_B,

$$0 \leqslant \alpha_1 < 1, \tag{4.3}$$

and the fluid velocities then become infinite as the lines $x \pm \eta y = 0$ are approached.

4.1. *Case* $\mu < \theta_B < \pi - \mu$

In this case, the diffracted waves given by (3.36) and (3.37) may be shown to be the same as those given by Robinson (1970). Since the reflected waves are the same, too, the two solutions are identical. The following discussion is therefore complimentary to that of Robinson.

Figure 3(*a*) shows the incident and reflected waves and these together give zero normal velocity on OA and on OB. Hence, so too must the diffracted waves alone. Thus, for a point $(x, 0)$ on OA, we have

$$\psi'_{\mathscr{D}+}(x \sin \mu) + \psi'_{\mathscr{D}-}(x \sin \mu) = 0 \quad (x > 0), \tag{4.4}$$

so that†

$$\psi'_{\mathscr{D}+}(s) = -\psi'_{\mathscr{D}-}(s) \quad s > 0. \tag{4.5}$$

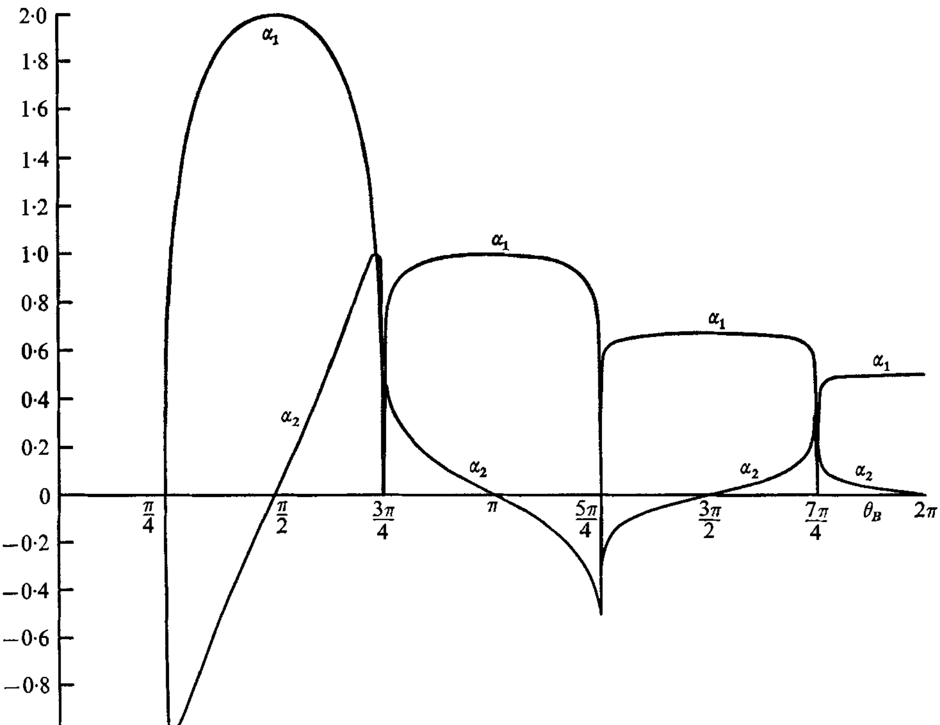

FIGURE 4. Values of $\alpha = \alpha_1 + i\alpha_2$.

Similarly, for a point $(r_B \cos \theta_B, r_B \sin \theta_B)$, on OB we have

$$\sin(\theta_B - \mu)\, \psi'_{\mathscr{D}+}(-r_B \sin[\theta_B - \mu]) - \sin(\theta_B + \mu)\, \psi'_{\mathscr{D}-}(r_B \sin[\theta_B + \mu]) = 0, \tag{4.6}$$

so that

$$\psi'_{\mathscr{D}+}(-s) = K\psi'_{\mathscr{D}-}(Ks) \quad (s > 0). \tag{4.7}$$

Equations (4.5) and (4.7) enable the complete diffraction field to be expressed in terms of $\psi'_{\mathscr{D}+}(\sigma_+)$ for negative values of its argument. This is depicted in figure 5,

† The relations (4.5) and (4.7) may of course be deduced analytically from (3.36) and (3.37).

where $\psi'_{\mathscr{D}_+}(-s)$ is denoted by $v(s)$. The total diffraction velocity is the vector sum of the three velocity fields that are depicted in the figure.

Values of $\psi'_{\mathscr{D}_+}$ for negative values of its argument and various values of θ_B in the range† $(\pi/2, \pi-\mu)$ are given in figure 6 where again we have taken $\mu = \pi/4$.

When inequality (4.2) is satisfied the results exhibit the remarkable property that was pointed out by Robinson (1970): namely,

$$\psi'_{\mathscr{D}_+}(0_-) = iU(1-K), \tag{4.8}$$

which is precisely minus the velocity at $\sigma_+ = 0_-$ due to $\psi_i + \psi_{\mathscr{R}AB}$ (see figure 3(*a*) and table 1). Also (4.5), (4.7) and (4.8) give

$$\psi'_{\mathscr{D}_+}(0_+) = iU(1-[1/K]), \tag{4.9}$$

which is minus the velocity due to $\psi_i + \psi_{\mathscr{R}BA}$. Hence, when (4.2) is satisfied, the total velocity is continuous across the line OC_1 of figure 3(*a*).

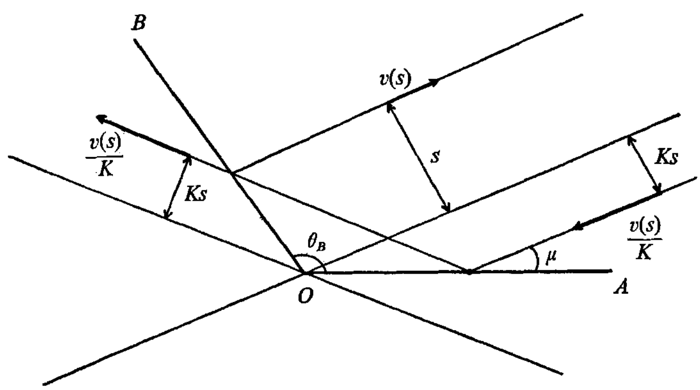

FIGURE 5. Structure of diffraction velocity field in case $\mu < \theta_B < \pi-\mu$.

Results are given in figure 6 to illustrate the behaviour as θ_B approaches $3\pi/4$ (the inclination of the characteristic $x+\eta y = 0$), as this behaviour is of practical as well as theoretical interest (Fofonoff 1967). It follows from (3.37) that

$$\lim_{\theta_B \to 3\pi/4} = \psi'_{\mathscr{D}_+}(\sigma_+) = -\int_0^\infty \frac{\exp(k\sigma_+ t)\,dt}{\log^2 t + \frac{3}{4}\pi^2 - \pi i \log t} \quad (\sigma_+ < 0), \tag{4.10}$$

and this is included in the figure. For (4.10) to be a good approximation, we must have

$$|\log(\tfrac{3}{4}\pi - \theta_B)| \ll 2\pi^2, \tag{4.11}$$

so that θ_B must be exceedingly close to $\frac{3}{4}\pi$. Results in figure 6(*b*) illustrate this point.

† Values for the range $(\mu, \frac{1}{2}\pi)$ may be deduced from those given in the figure by using the relation,

$$\{\psi'_{\mathscr{D}_+}(\sigma_+)\}_{\theta_B=\frac{1}{2}\pi-\Delta} = \frac{1}{K_\Delta}\left\{\psi'^{*}_{\mathscr{D}_+}\left(\frac{\sigma_+}{K_\Delta}\right)\right\}_{\theta_B=\frac{1}{2}\pi+\Delta}, \quad (\sigma_+ < 0),$$

where $K_\Delta = \dfrac{\sin(\frac{3}{4}\pi+\Delta)}{\sin(\frac{1}{4}\pi+\Delta)}$ and the asterisk denotes the complex conjugate.

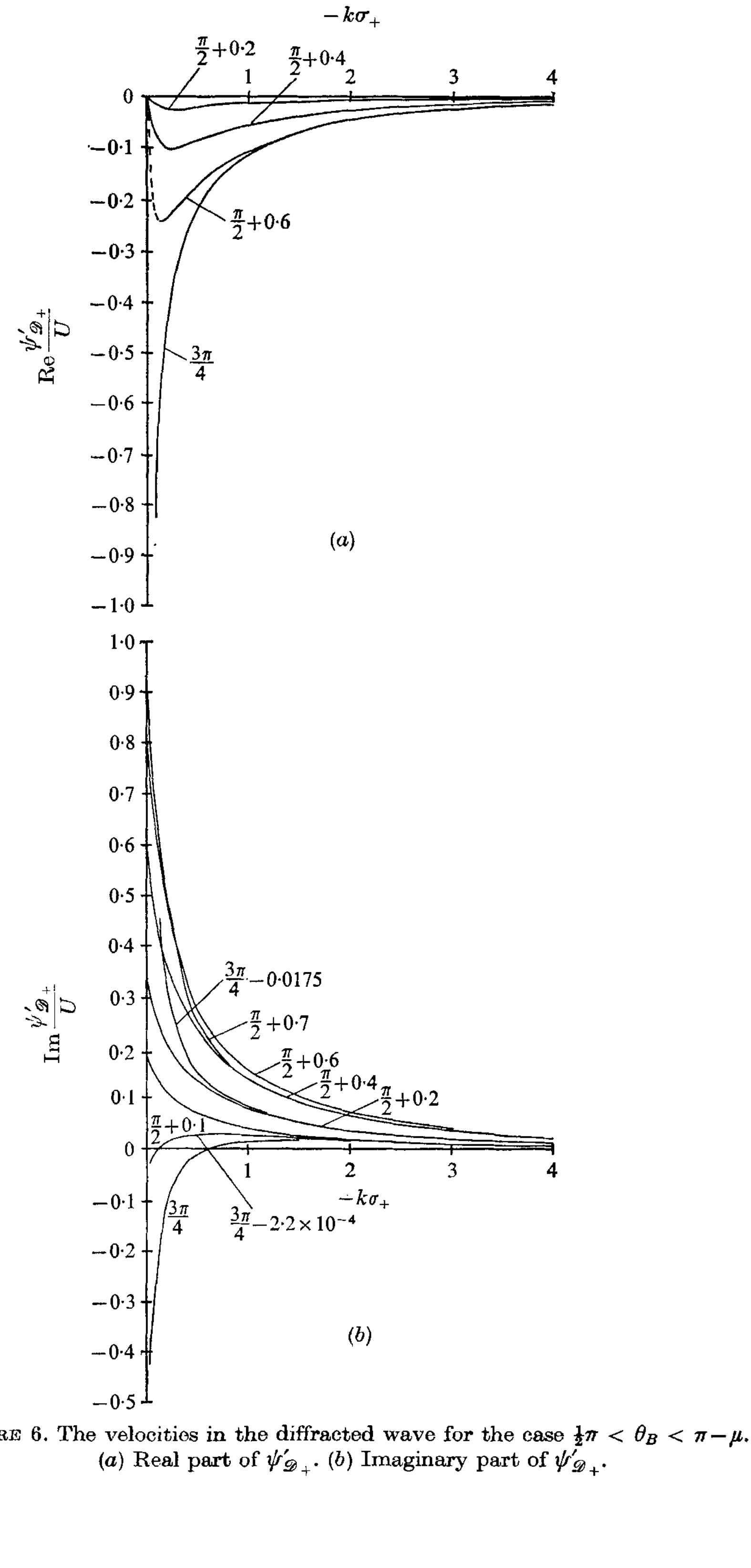

FIGURE 6. The velocities in the diffracted wave for the case $\frac{1}{2}\pi < \theta_B < \pi-\mu$. (a) Real part of $\psi'_{\mathscr{D}+}$. (b) Imaginary part of $\psi'_{\mathscr{D}+}$.

4.2. *Case* $\pi-\mu < \theta_B < \pi+\mu$

In this case the velocity due to the reflected waves is continuous across the line OC_1 of figure 3(*b*), but nevertheless there exists near it a diffracted wave whose velocities are given in figure 7 for various values of θ_B in the range† $(\pi-\mu, \pi)$. Relations (4.5) and (4.7) hold and give $\psi'_{\mathscr{D}-}(\sigma_-)$ in terms of the results given.

Using equation (A 13) of the appendix we may calculate the increase in the energy flux in the direction OC_1, $\Delta\bar{P}_{C_1}$, due to diffraction, and the results are given in figure 8. Diffraction leads to a positive backscatter of energy that increases as θ_B approaches $\frac{3}{4}\pi$.

4.3. *Case* $\theta_B = 2\pi$

In this case, the internal wave is incident on a knife edge as shown in figure 9, and there will be diffracted waves near each of the lines OC_1, OC_2, OC_3 and OC_4. Equation (2.24) gives

$$C = -4\pi i, \tag{4.12}$$

and we find that the velocities in the diffracted waves can be expressed in terms of Fresnel integrals. For the diffracted wave near OC_1, we find that

$$\psi'_{\mathscr{D}+}(\sigma_+) = -\psi'^{*}_{\mathscr{D}+}(-\sigma_+) = -\frac{U}{2}\left\{f(x)-\frac{1}{\pi x}-g(x)-i\left[f(x)-\frac{1}{\pi x}+g(x)\right]\right\}, \quad (\sigma_+ > 0)$$

where $x = \sqrt{(2k\sigma_+/\pi)}$,

$$\left.\begin{aligned} f(x) &= [\tfrac{1}{2}-S(x)]\cos\left(\frac{\pi x^2}{2}\right)-[\tfrac{1}{2}-C(x)]\sin\left(\frac{\pi x^2}{2}\right), \\ \text{and} \quad g(x) &= [\tfrac{1}{2}-C(x)]\cos\left(\frac{\pi x^2}{2}\right)+[\tfrac{1}{2}-S(x)]\sin\left(\frac{\pi x^2}{2}\right). \end{aligned}\right\} \tag{4.13}$$

(See Abramowitz & Stegun 1964, § 7.) These values of $\psi'_{\mathscr{D}+}$ are given in figure 10.

We also find that the diffraction velocities near OC_4 are the same as those near OC_1, i.e. that near OC_4,

$$\psi'_{\mathscr{D}-}(s) = \psi'_{\mathscr{D}+}(s), \tag{4.14}$$

where $\psi'_{\mathscr{D}+}$ is given by (4.13). For the wave near OC_3, the velocities for negative values of σ_+ are the same as those in the wave near OC_1 for negative values of σ_+. Also, the velocities near OC_3 for σ_+ positive are related to those near OC_4 for σ_- positive by the condition that together they should give zero normal velocity on OB. The velocities in the wave near OC_2 may be obtained in a similar manner.

Equation (4.14) implies that the diffracted waves near OC_1 and OC_4 radiate the same power, and (4.13) and equation (A 13) of the appendix show that this power is

$$\begin{aligned} \Delta\bar{P} &= -\frac{\eta\rho_0\omega U^2}{2k^2}\int_0^\infty \{\pi\xi[f^2(\xi)+g^2(\xi)]-f(\xi)\}\,d\xi \\ &= 0{\cdot}080\eta\frac{\rho_0\omega U^2}{k^2}, \end{aligned} \tag{4.15}$$

† Values for the range $(\pi, \pi+\mu)$ may be deduced by using the relation,

$$\{\psi'_{\mathscr{D}+}(s)\}_{\theta_B=\pi+\Delta} = -\{\psi'^{*}_{\mathscr{D}+}(-s)\}_{\theta_B=\pi-\Delta}.$$

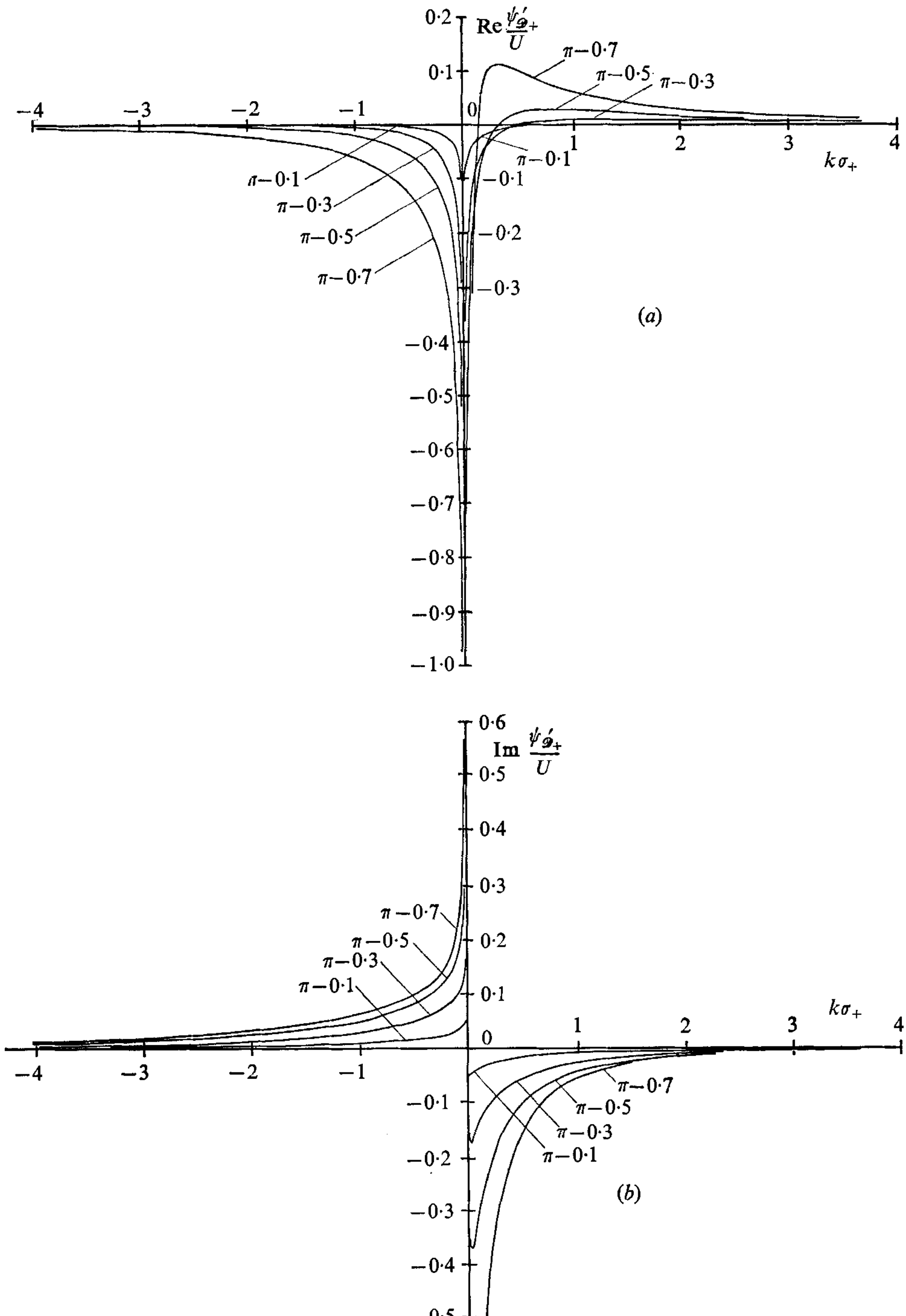

FIGURE 7. The velocities in the diffracted wave for the case $\pi - \mu < \theta_B < \pi$. (a) Real part of $\psi'_{\mathscr{D}+}$. (b) Imaginary part of $\psi'_{\mathscr{D}+}$.

approximately, for general values of μ. For comparison, the power in the incident wave per unit length normal to the group velocity is $\eta\rho_0\omega U^2/2k$, so that the length in this direction that contains a power equal to that radiated in either of the directions OC_1 and OC_4 is 0·05 wavelengths, approximately.

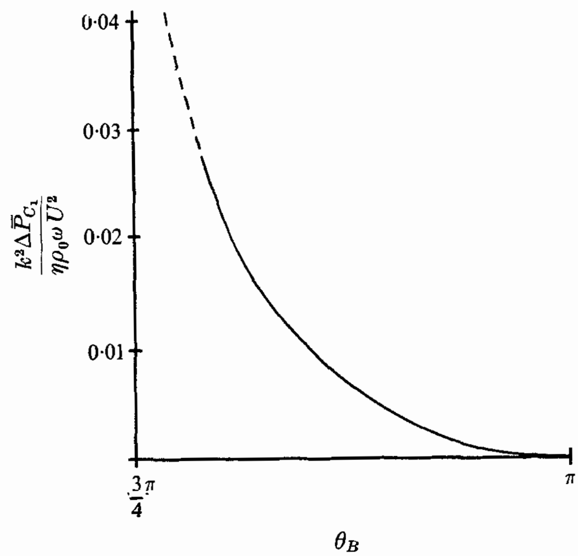

FIGURE 8. Backscatter of energy for case $\pi-\mu < \theta_B < \pi$.

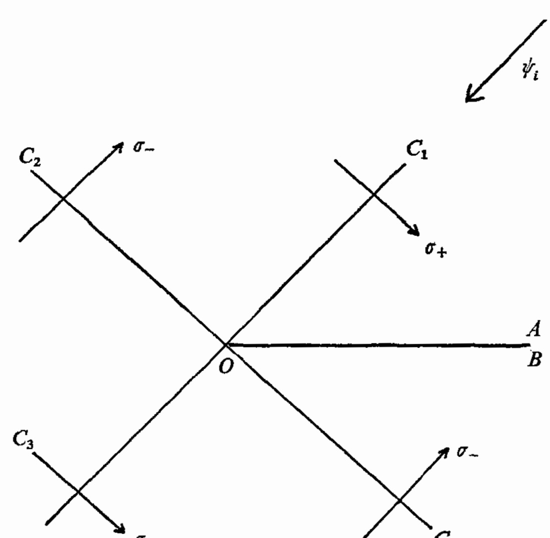

FIGURE 9. Notation for case $\theta_B = 2\pi$.

While this paper was being revised, Barcilon & Bleistein (1969) gave a solution to a problem closely related to that considered in this section. Their equation (3.16) gives the stream function for the diffraction of an inertial wave by a knife-edge; and, using results in Ambramowitz & Stegun (1967, §7), we find it represents a motion very similar to that given by our (4.13).

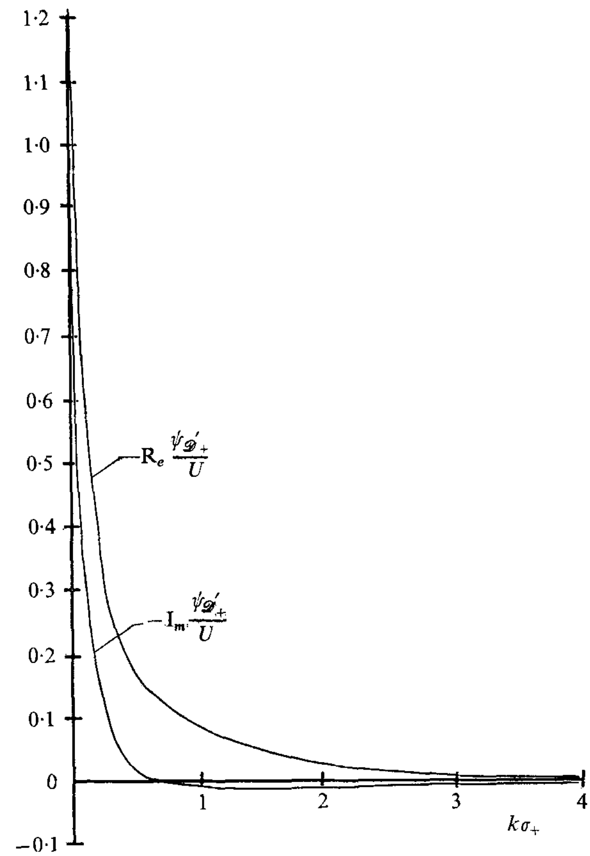

FIGURE 10. The velocities in the diffracted wave near OC_1 for the case $\theta_B = 2\pi$.

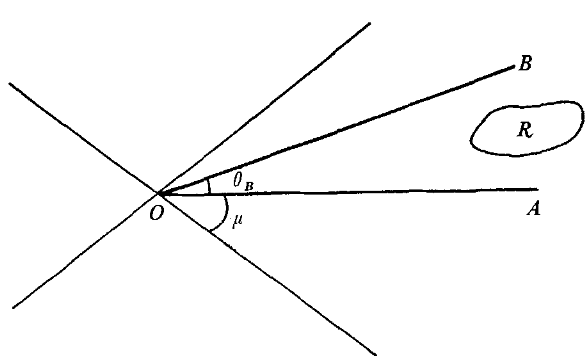

FIGURE 11. Problem considered in the case $0 < \theta_B < \mu$.

5. The case $0 < \theta_B < \mu$

In this case, it is convenient to consider the motion produced by oscillatory forces ($X \exp[-i\omega t]$, $Y \exp[-i\omega t]$) that act throughout a region R as shown in figure 11. The stream function of the motion is given by (2.21) in which ψ_V is given by (2.28).

Consider a point (x, y) close to (x_S, y_S). Let

$$x = x_S + x', \quad y = y_S + y', \tag{5.1}$$

so that x'/r_S and y'/r_S are small, where

$$r_S = (x_S^2 + y_S^2)^{\frac{1}{2}} \tag{5.2}$$

is the distance from the disturbance point (x_S, y_S) to the vertex of the wedge. Then (2.28) becomes approximately

$$\psi_V = \frac{1}{4\pi\omega\eta} \log\{(x + \eta y - x_S - \eta y_S)(x - \eta y - x_S + \eta y_S)\} + \text{const.}, \tag{5.3}$$

which we recognize as a constant multiple of the stream function for an oscillatory vortex in an unbounded region. (See Hurley 1969, (3.18).) Hence, if the region R is small, the motion near it will be approximately the same as if the walls were absent. In particular, for a small, rigid oscillating body, one quarter of the power-output will be radiated in each of the four characteristic directions from it.

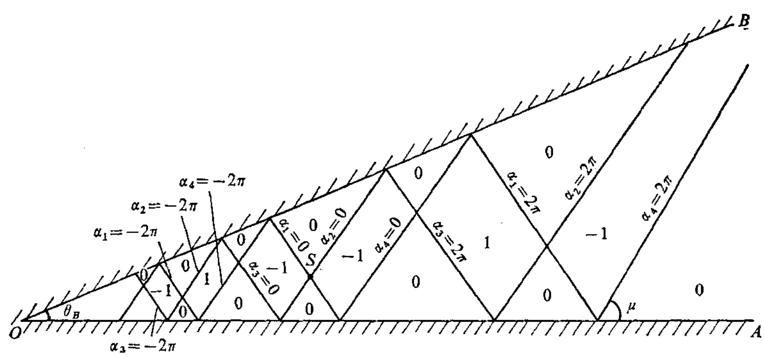

FIGURE 12. Imaginary part of $4\omega\eta\,\psi_V$ for case $0 < \theta_B < \mu$.

Far from the small body the accurate expression (2.28) for ψ_V must be used. Calculations show that its imaginary part is piecewise constant, and takes the values given in figure 12. From this figure, it is clear that (2.28) correctly represents the repeated reflexion of energy at the walls OA and OB. Hence, one half of the power output of the body will eventually arrive at O, where there must therefore be an energy sink. This conclusion has also been reached by Greenspan (1969).

It is also clear that the problem posed in §3 is inappropriate in the present case. This is because the amplitude of the incident wave was taken to be finite, which leads to an infinite influx of energy from infinity. To transmit this energy to O, infinite velocities would be needed at all points a finite distance from O (see the appendix). Wunsch (1969) considered the motions corresponding to the eigensolutions R_n given by (2.26) for n positive. In these solutions, the wave amplitude tends to zero at infinity, so that the above difficulty does not arise.

6. Limitations of ray theory for internal waves

The above investigation makes clear certain limitations of the so-called ray theory for internal waves, in which only the incident and reflected waves are considered. To illustrate these limitations, we reconsider a problem treated by Longuet-Higgins (1969)† using ray theory methods. The problem is that of an internal wave incident on the simple saw-tooth roughness shown in figure 13(*a*), in the case when the slope of the faces is less than the slope of the characteristics. Since all the reflected waves are inclined to the left, there will be no back-scatter of energy at all, according to the ray theory.

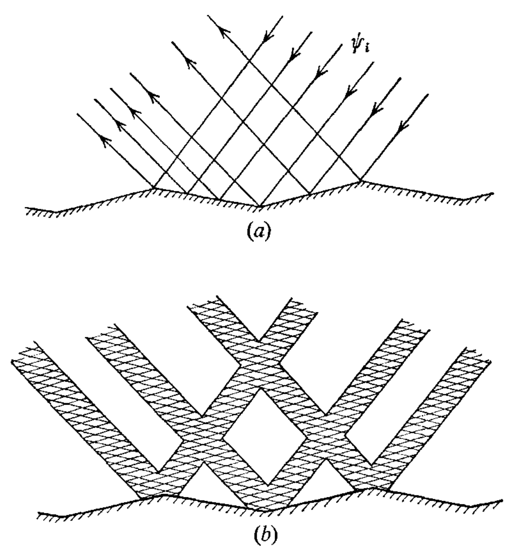

FIGURE 13. Internal wave incident on simple saw-tooth roughness. (*a*) Incident and reflected waves. (*b*) Regions in which diffracted waves are important.

However, our investigation shows that, for an isolated corner, the diffracted waves will be as important as the incident and reflected ones at all points within a quarter wavelength or so of either characteristic that passes through the corner. Further, this theory can be applied to the saw-tooth problem, provided the length scale of the roughness is large enough to prevent the overlapping of neighbouring regions in which diffraction effects are important. This situation is depicted in figure 13(*b*); the diffraction regions occupy a sufficient fraction of the total for their effect to be significant. The results of §§4.2 and 4.3 show that they give a positive back-scatter of energy, and this is consistent with the results of theories for roughness elements of general shape and small height. (See Cox & Sandstrom 1962; Hurley & Imberger 1969.)

If the length scale of the roughness is much larger than the wavelength, the regions in which diffraction is important will only be a small fraction of the total. The over-all effects of diffraction will be small, and the ray theory approximately

† Published while the present paper was being revised.

correct. On the other hand, if the length scale of the roughness is of the same order as, or smaller than, the wavelength diffraction effects will be important everywhere, and the ray theory as given by Longuet-Higgins will be unsatisfactory. The conditions for the ray theory to hold in this and similar problems are therefore like those for the applicability of the geometrical theory of optics. In both cases, the length scales in the problem must be much larger than the wavelength.

Appendix. Calculation of energy flux

Consider a curve of length l joining any two points P and Q that lie in the fluid. Let q_n be the normal velocity from right to left at any point on the curve, and let p be the fluid pressure. Then the time average of the rate, at which the fluid to the right of the curve does work on the fluid to the left of it, is

$$\overline{P}_{PQ} = \frac{1}{4}\int_0^l (pq_n^* + p^* q_n)\, ds, \tag{A 1}$$

where s is the arc-length. We shall refer to $\overline{P}_{PQ}$ as the energy-flux in the sense of q_n.

If
$$\psi = F_+(\sigma_+) + F_-(\sigma_-), \tag{A 2}$$

then the integration of the linearized equations of motion gives

$$p = i\eta\rho_0\omega(F_+(\sigma_+) - F_-(\sigma_-)) + C, \tag{A 3}$$

where C is an arbitrary constant that we take to be zero.

Equations (A 1) to (A 3) now give

$$\overline{P}_{PQ} = \frac{i\eta\rho_0\omega}{4}\int_{AB} \{[F_+F_+'^* - F_+^* F_+']\, d\sigma_+ + [F_-^* F_-' - F_- F_-'^*]\, d\sigma_-\} - \frac{\eta\rho_0\omega}{2}\left\{\mathrm{Im}\left[F_+(\sigma_+)\, F_-^*(\sigma_-)\right]_P^Q\right\}. \tag{A 4}$$

Now, let P and Q be two points at either end of a long line, $\sigma_- =$ constant, which cuts the line OC_1 of figure 3 (*b*) at a large distance from O. Then, on PQ,

$$\psi = \psi_i(\sigma_+) + \psi_{\mathscr{R}A}(\sigma_-) + \psi_{\mathscr{D}_+}(\sigma_+), \tag{A 5}$$

approximately. Also, if we select P and Q to satisfy

$$\psi_i(\sigma_{+P}) = \psi_i(\sigma_{+Q}), \tag{A 6}$$

then (A 4) simplifies to

$$\overline{P}_{PQ} = -\frac{\eta\rho_0\omega}{2}\,\mathrm{Im}\int_{PQ} F_+ F_+'^*\, d\sigma_+, \tag{A 7}$$

where
$$F_+(\sigma_+) = \psi_i(\sigma_+) + \psi_{\mathscr{D}_+}(\sigma_+), \tag{A 8}$$

and $\bar{P}_{PQ}$ is positive for an energy flux in the sense of OC_1. Thus,

$$\bar{P}_{PQ} = -\bar{P}_i - \eta\rho_0\omega U \operatorname{Re}\int_{-\infty}^{\infty} \exp(ik\sigma_+)\,\psi_{\mathscr{D}_+}\,d\sigma_+ - \frac{\eta\rho_0\omega}{2}\operatorname{Im}\int_{-\infty}^{\infty}\psi_{\mathscr{D}_+}\psi'^{*}_{\mathscr{D}_+}\,d\sigma_+, \tag{A 9}$$

where

$$\bar{P}_i = \frac{\eta\rho_0\omega U^2}{2k}\int_{PQ} d\sigma_+, \tag{A 10}$$

and is thus the energy flux associated with the incident wave.

Integration by parts shows that the second term in (A 9) is

$$\frac{\eta\rho_0\omega UI}{k},$$

where

$$I = \int_{-\infty}^{\infty}\exp(ik\sigma_+)\,\psi'_{\mathscr{D}_+}\,d\sigma_+. \tag{A 11}$$

Using (3.37) and carrying-out the integration with respect to σ_+, we find

$$\begin{aligned} I &= \frac{U}{Ck}\sinh\frac{2\pi^2}{C}\int_0^{\infty}\frac{dt}{(t+i)\{\cos([\pi/C][2\log t - i\pi]) - \cosh[2\pi^2/C]\}} \\ &\quad - \frac{U}{Ck}\sinh\frac{2\pi^2}{C}\int_0^{\infty}\frac{dt}{(t-i)\{\cos([\pi/C][2\log t + i\pi]) - \cosh[2\pi^2/C]\}} \\ &= -\frac{U}{Ck}\sinh\frac{2\pi^2}{C}\int_{-i\infty}^{i\infty}\frac{dz}{(z+1)\{\cos([\pi/C][2\log z]) - \cosh[2\pi^2/C]\}}. \end{aligned} \tag{A 12}$$

Since the integrand in (A 12) is regular in the right-half-plane, it follows by Cauchy's theorem that $I = 0$. Thus, the second term in (A 9) is zero, and the change in the energy flux across PQ in the direction of OC_1, due to the diffracted wave, is

$$\Delta\bar{P}_{C_1} = -\frac{\eta\rho_0\omega}{2}\operatorname{Im}\int_{-\infty}^{\infty}\psi_{\mathscr{D}_+}\psi'^{*}_{\mathscr{D}_+}\,d\sigma_+. \tag{A 13}$$

REFERENCES

Ambramowitz, M. & Stegun, I. A. 1967 *Handbook of Mathematical Functions*. National Bureau of Standards.

Barcilon, V. & Bleistein, N. 1969 *Studies Appl. Maths.* **48**, 91–104.

Bers, L., John, F. & Schechter, M. 1964 *Partial Differential Equations*. New York: Interscience.

Cox, C. S. & Sandstrom, H. 1962 *J. Ocean. Soc. Japan, 20th Anniver. Vol.*, pp. 499–513.

Fofonoff, N. P. 1967 *Proc. IAPO Symposium on Internal Waves, General Assembly of IUGG, Berne, Switzerland.*

Greenspan, H. P. 1969 *Studies Appl. Maths.* **48**, 19–28.

Hurley, D. G. 1969 *J. Fluid Mech.* **36**, 657–72.

Hurley, D. G. & Imberger, J. 1969 *Bull. Austr. Math. Soc.* **1**, 29–46.

Lamb, H. 1932 *Hydrodynamics*. Cambridge University Press.

Larson, L. 1969 *Deep Sea Res.* **16**, 411–419.

Longuet-Higgins, M. S. 1969 *J. Fluid Mech.* **37**, 231–50.

Phillips, O. M. 1966 *The Dynamics of the Upper Ocean*. Cambridge University Press.

Robinson, R. M. 1969 *Deep Sea Res.* **16**, 421–9.

Robinson, R. M. 1970 *J. Fluid Mech.* **42**, 257–68.

Sagan, H. 1961 *Boundary and Eigenvalue Problems in Mathematical Physics*. New York: John Wiley.

Wunsch, C. 1968 *Deep Sea Res.* **25**, 251–8.

Wunsch, C. 1969 *J. Fluid Mech.* **35**, 131–44.